Quality Glass Processing by Laser Induced Backside Wet Etching

Z. Q. Huang[*,**,***], M. H. Hong[*,**], K. S. Tiaw[**] and Q. Y. Lin[***]

[*]*Department of Electrical and Computer Engineering, National University of Singapore, 4 Engineering Drive 3, Singapore 117576*
[**] *Data Storage Institute, 5 Engineering Drive 1, Singapore 117608*
HONG_Minghui@dsi.a-star.edu.sg
[***] *Chartered Semiconductor Manufacturing Ltd., 60 Woodlands Industrial Park D, Street 2, Singapore 738406*

Laser Induced Backside Wet Etching (LIBWE) technique is applied for quality microprocessing of quartz. A direct-write approach is chosen to etch structures directly onto quartz. A diode pumped solid state (DPSS) 3rd harmonic Nd:YAG laser with a wavelength of 355 nm is used. High speed etching of glass is successfully carried out at a repetition rate of 10 kHz and a scanning speed of 100 mm/s using a galvanometer. With high speed processing, the amount of processing time is reduced greatly. Microfluidic channels are created by this technique within a short time. 3D surface scan shows that they are of good cross-sectional uniformity. Deposits are observed on the glass surface after the laser processing. X-ray photoelectron spectroscopy (XPS) analyses further reveal that this deposit is carbon related. Laser cleaning is applied to remove the contamination.
DOI: 10.2961/jlmn.2007.03.0006
Keywords: LIBWE, glass processing, laser etching, microfabrication, wet etching

1. Introduction

Quartz has excellent properties, such as high transparency in a wide wavelength range, strong scratch resistance, high thermal and chemical stabilities. This makes quartz suitable for a wide area of applications. However, it is difficult to etch well-defined structures on quartz glass, especially crack-free structures. This poses a technical challenge to fabricate micro-sized structures on the surface of the quartz. Conventional lithography is time-consuming and expensive. Methods of direct laser ablation are limited to photon-absorbing materials [1-3]. Furthermore, direct laser ablation produces cracks, damages and undesirable roughness to the etched surfaces, making it unsuitable for critical applications. An alternative method to etch glass is to use Laser Induced Backside Wet Etching (LIBWE) [4]. This technique does not require the laser energy to be absorbed by the glass to induce etching. Instead, it is the absorbing liquid which absorbs the laser energy and induces etching. The LIBWE method provides a fast and accurate way to etch structures in quartz, using a laser and an absorbing liquid. LIBWE enables micro-fabrication without cracks formation [4-11] at atmospheric pressure and simplification of pre/post treatment of substrate. This means that LIBWE can be carried out relatively easily at room temperature and pressure. As the method is able to direct-write on glass, through the use of computer numerical control (CNC) programming, this also makes the LIBWE technique flexible and suitable for fast prototyping of samples as well as for small scale production. Furthermore, various types of lasers [4-11] can be used for LIBWE.

In this study, we investigate the feasibility of using a much higher pulse repetition rate diode pumped solid state (DPSS) laser for high speed quality microprocessing of quartz. The laser is a Nd:YAG laser at 3rd harmonic with a wavelength of 355 nm. It is a UV laser which is widely used in the industry due to its comparatively lower maintenance cost, better stability, higher repetition rate and power output as compared to excimer lasers. The effect of the absorbing liquids on the process is examined by analyzing the absorption spectra of the absorbing liquids. Generation of by-products is observed and their chemical compositions are studied using X-ray photoelectron spectroscopy (XPS). Laser cleaning techniques are employed to remove the contamination. The LIBWE process is used to fabricate some microfluidic channels by high speed laser processing and CNC programming.

2. Experimental

Figure 1 shows the schematic diagram of the experimental setup. The laser used is a COHERENT AVIA laser, which is a Nd:YAG DPSS laser with the 3rd harmonic generation of a wavelength of 355 nm and a full width at half maximum (FWHM) pulse width of 30 ns. It has a high repetition rate in the range from 1000 Hz to 20000 Hz. A galvanometer is used for high speed laser processing, at a fast scanning speed of 100 mm/s. CNC programming controls the direction of the laser scans to achieve direct-writing on the quartz. The quartz substrate is a Photonik UV quartz substrate with a diameter of 3 inches and a thickness of 1 mm. The absorbing liquid used is pure toluene from Merck and mixed with pyrene to a concentration of 0.4 M. The surface profile is taken using a surface profiler, Surftest SV-3000 from Mitutoyo. The chemical composition is analyzed using XPS, Quantera SXM from PHI. The absorption spectra of toluene and pyrene dissolved in toluene are measured using UV-Vis system UVPC spectrophotometer.

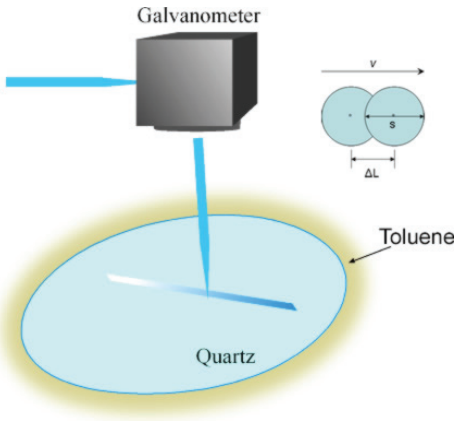

Fig. 1. Schematic diagram of the experimental setup. A galvanometer is used for high speed processing of the quartz.

3. Results and Discussion

3.1 Effects of absorbing liquid

Figure 2 shows the absorption spectra of toluene and pyrene dissolved in toluene at a concentration of 0.4 M. It shows that toluene absorbs light in the 355 nm wavelength region very weakly. The cut-off absorption is about 300 nm. In contrast, toluene absorbs very well in the region below 300 nm, which corresponds to the wavelengths used in various studies [4-12]. To increase the absorption of the irradiating 355 nm light, pyrene is added to toluene. In Fig. 2, the absorption of the mixture of pyrene and toluene shows that by adding pyrene to toluene, the absorption of 355 nm light is greatly enhanced and the cut-off absorption is extended to about 500 nm. Increasing the absorption of the liquid is desirable as the etch rate increases with the absorption coefficient [9]. As the maximal depth of the melted quartz layer depends on the absorption coefficient of the solution [9], a higher absorption coefficient results in deeper melted quartz depth, and the melted quartz is subsequently removed by various mechanisms [4-10]. With better absorption of the irradiating light, more quartz will be melted to produce deeper etch depth, resulting in a higher etch rate.

Figure 3 illustrates the relation between the achieved etched depth and laser fluence, and compares the differences when using toluene alone and the mixture of pyrene and toluene, at a repetition rate of 10 kHz and a scanning speed of 100 mm/s. The laser spot size was measured using a piece of thermal paper (~ 100 μm). Laser pulse energy is varied and laser fluence was calculated by dividing the laser pulse energy with the area of the laser spot. The number of beam overlaps can be determined as:

$N = \frac{s}{v} RR$, where N is the number of beam overlaps, s the beam spot size, v the scanning speed and RR the repetition rate. There are around 10 pulses of laser overlaps at a repetition rate of 10 kHz and a scanning speed of 100 mm/s. At a same laser fluence, using the mixture of pyrene and toluene achieves a much deeper etched depth as compared to using toluene only. A laser fluence of 1.5 J/cm^2 attains an etched depth of 250 nm when using toluene alone. At the same laser fluence, an etched depth of 1350 nm is achieved with the mixture of pyrene and toluene. This is about five times increase in the etch rate. Furthermore, the etched depth increases non-linearly with the laser fluence. As a result, the mixture of pyrene and toluene has an even higher etch rate than toluene at higher laser fluences. This is advantageous for the rapid processing. Meanwhile, the threshold fluence needed to initiate the laser etching is also lowered with the addition of pyrene. From the extrapolation of the fitted curves in Fig. 3, the threshold fluence in toluene is about 1.1 J/cm^2 while the threshold fluence in the mixture of pyrene and toluene is only 0.4 J/cm^2. The lower threshold fluence is because the pyrene and toluene mixture has a higher absorption of 355 nm light than toluene alone. A liquid with a higher absorption coefficient has a shorter light penetration depth, resulting in decreased heated liquid volume and higher temperature [7]. Subsequently, this permits the pyrene and toluene mixture to yield a higher etch rate than using toluene alone. Using the 355 nm laser, the achieved etching threshold is lower than that achieved by using LIBWE of visible light laser at 532 nm [11].

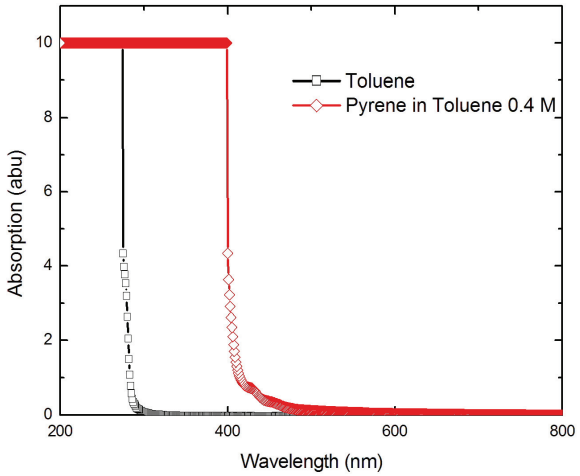

Fig. 2. Absorption spectra of toluene and pyrene mixed in toluene. Absorption at 355 nm is quite weak for toluene but the absorption at 355 nm for pyrene mixed in toluene in a concentration of 0.4 M is much stronger.

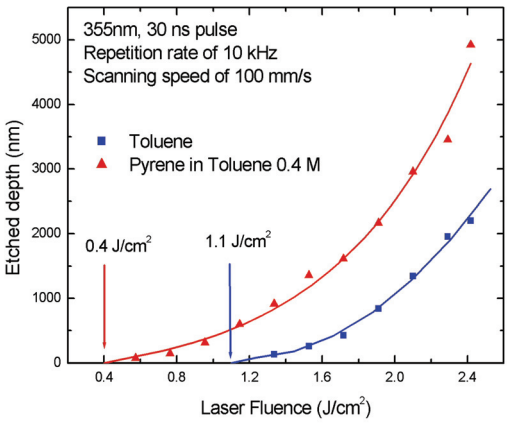

Fig. 3. Comparison of the etched depth created by LIBWE in different absorbing liquids.

Figure 4 shows the various etched profiles obtained at a laser fluence of 0.90, 0.96, 1.18, 1.42, 1.52 and 1.70 J/cm^2 in toluene alone. At 0.90 J/cm^2, there is almost no modification to the surface but as the laser fluence is slowly increased to 0.96 J/cm^2 and then to 1.18 J/cm^2, shallow but observable trenches are etched into the surface. The increase of laser fluence from 1.18 to 1.42 J/cm^2, from 1.42 to 1.52 J/cm^2, and from 1.52 to 1.70 J/cm^2 results in an increase of 20 nm, 120 nm and 184.6 nm in the etched depth respectively. With an increase of 0.1 J/cm^2 in laser fluence from 1.42 to 1.52 J/cm^2, it leads to an increase over 100 nm in the etched depth. In comparison, an increase of 0.24 J/cm^2 from 1.18 J/cm^2 to 1.42 J/cm^2 results in only 20 nm increase in the etched depth. This illustrates the non-linear relation between the etched depth and laser fluence.

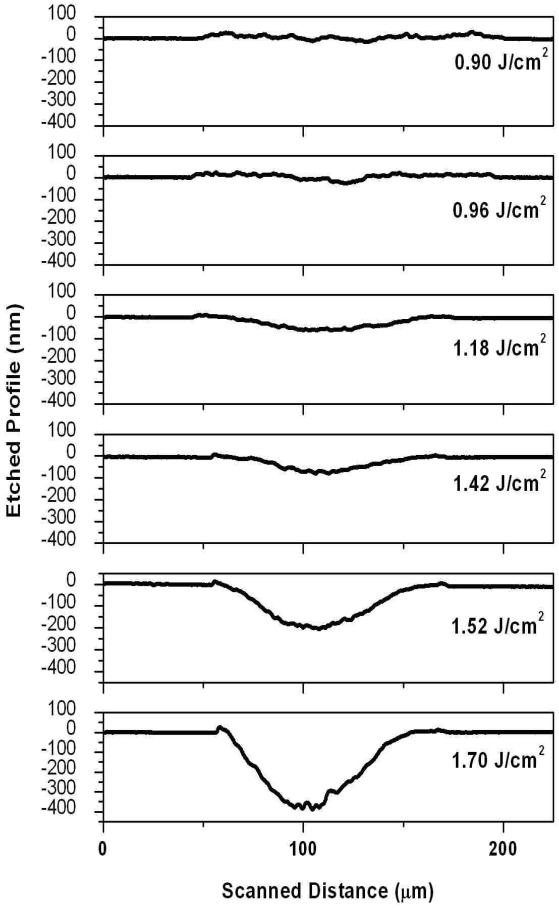

Fig. 4. Various depth profiles obtained in a single laser scan with varying laser fluence.

3.2 Microfluidic channel fabrication

In recent years, there is a rapid growing interest in the technologies and market trends of microfluidic chips. The attraction of such chips is their small sizes and high throughput in analysis work. Also, microscopic channels have different properties from macroscopic counterparts, such as having laminar flow properties and different fluidic resistances. There are various types of materials suitable for the channel fabrication, with glass, silicon and polymer as the main substrate materials. The stability of glass to chemical reactions and the transparency of glass for visual observation of processes make it an attractive candidate to manufacture biochips on.

In this work, LIBWE is used to etch trench structures on quartz, which can be used in microfluidics. The designs are based on the idea of droplet manipulation and droplet fission [13], and groove structures for enhanced mixing in microfluidic channels [14]. In the former case, as a droplet flow towards a bifurcating junction, the fluidic flow towards the left and right channels creates a fluidic pressure on the droplet. Based on the geometries of the spilt channels, the amount of fluid flowing to the left and the right can either be similar or different. The fluidic pressure on the droplet can thus be varied through different geometries of the channels. Droplets of smaller sizes can be spilt off from the main droplet, with similar or dissimilar sizes which depend on the channel geometries. For example, if both the left and right channels are of the same size, then the amount of fluid following into both channels would be similar. The pressure exerted on the droplet is thus split evenly and two droplets of similar sizes can be created, with one going to the right channel and the other to the left. This allows the control of the fission of the droplets. In the latter case, due to the groove placement in the path of the fluidic, there is increased lateral perturbation in the stream flow. This leads to the creation of rotating vortices in the liquid, and thus enhances mixing of the fluid.

Figure 5a shows the 3D profiles of a microfluidic structure created by high speed LIBWE processing at a repetition rate of 10 kHz and a fast scanning speed of 100 mm/s. The surface profile is obtained using a surface profile which probes progressively in x and y directions. The measured area is 2.00 mm by 1.80 mm. At the bifurcating junctions, there are a few spots of slightly deeper etched depths. This is most probably because at those junctions, the light path has to take a turn, and consequently decelerating and re-accelerating at those areas. This results in a slightly longer dwelling time of the light at those places and hence causes those areas to receive slightly more etching. The issue can be solved by programming a faster turning speed or shortening the processing time at those junctions. The cross-sectional view horizontally across the surface is displayed and shows the Gaussian profiles of the trenches. The Gaussian surface profile is due to the Gaussian beam profile of the laser. In the magnified view of the respective four trenches, they have similar color-coded profiles, showing that all of them are similar in the etched depth. Furthermore, the widths of the four channels are 30 ± 1 μm. This shows good geometrical control of the etched channels in achieving equally sized channels. For this particular intended application, the similar sized channels would split off similar sized daughter droplets from the main droplet, since the amounts of fluid flowing into the channels are similar. Figure 5b shows the 3D zoom-in view of the bifurcating channel junction. The picture is tilted to show the bottom edges of the channels. The bottom is color-coded blue throughout, showing the good uniformity of the etched depth. The 3D scan also shows that the edges are straight, crack-free and of low distortion and roughness.

Figure 6 shows groove protrusions on quartz surface. These structures are created by milling away the surrounding quartz, creating isolated structures in the

middle of the channel. These structures can aid in enhancing [14] the mixing of reagents as they pass through the microfluidic channels.

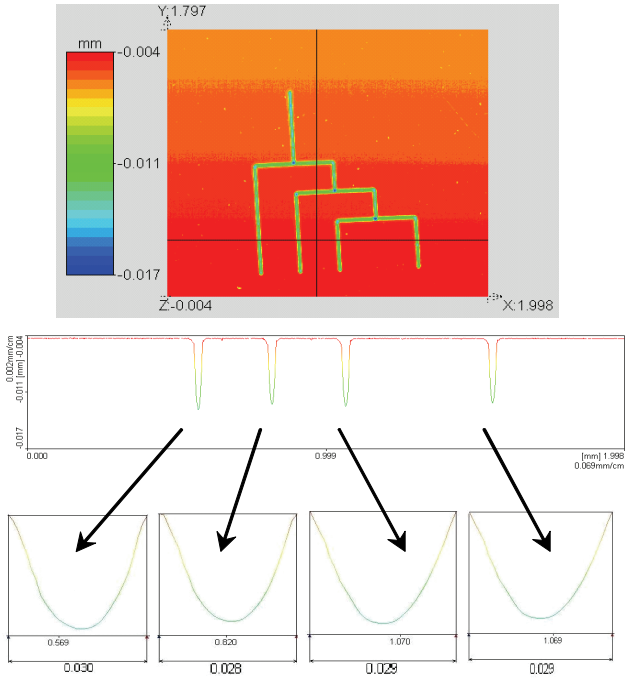

Fig. 5a. Profile scan of the microfluidic channel.

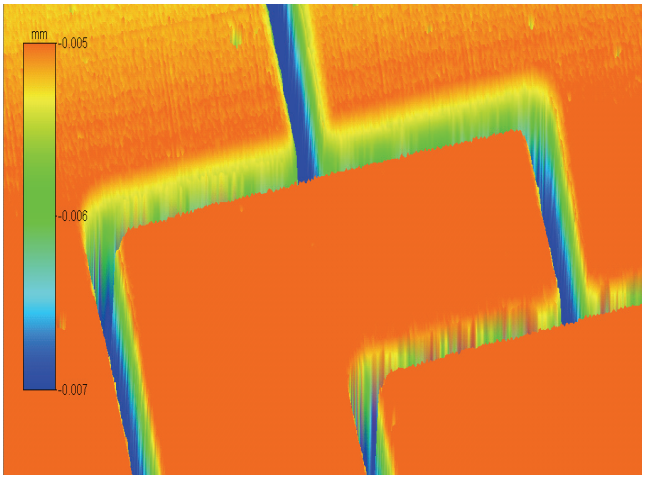

Fig. 5b. Zoomed 3D view of the bifurcating junctions.

3.3 By-products formation and removal

During processing of the quartz using LIBWE, upon repeated irradiation, the production of black by-product particles is observed. Optical inspection of the processed surface shows strong adherence of these particles to the surface of the quartz. XPS analysis is carried out to examine the chemical compositions of the contaminants. The elements present are C, O, and Si. Figures 7a to 7c show the individual narrow-range scans for the individual elements, with the appropriate curves fitted.

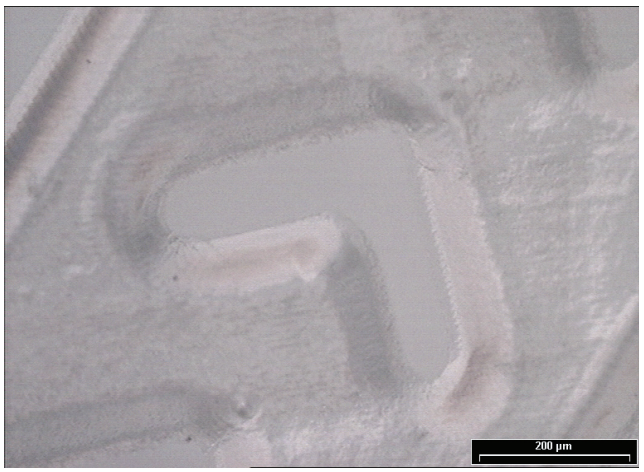

Fig. 6. Picture of a quartz groove created in the middle of the channel.

Carbon has three states and is deduced that the carbon has a C-C / C-H bond at a binging energy of 284.65 eV, a C-O bond at 286.19 eV and a C=O bond at 288.94 eV. O has three states. The binding energy of 531.07 eV could be due to OH group. The binding energy of 532.51 eV corresponds to the O-Si bond found in the quartz and the O-C bond, while it is the O=C bond at 533.17 eV. Si has a binding energy of 103.18 eV and this corresponds to the Si-O bonds in quartz. From all this data, it can be interpreted that the contamination is of carbon nature as carbon is the foreign element. The carbon is most probably due to the decomposition of the absorbing liquids. Upon continual irradiation of laser pulses, the absorbing liquid repeatedly goes through cycles of laser absorption and heat release [15]. This could have caused the decomposition of the organic molecules, producing the carbon by-products which are subsequently deposited onto the surface during etching.

The carbon adheres stubbornly to the substrate surface and is difficult to be removed by conventional ultra-sonic cleaning. In this work, laser cleaning is used to remove the carbon contamination. The contaminated surface is cleaned by overlapping laser pulses on the quartz surface in air (without the liquid for the glass etching) using the same 355 nm laser source, but at a lower laser fluence of 0.50 J/cm^2. The carbon particles are held to the surface by adhesion forces, such as van der Waals' force or chemisorbed onto the surface by forming chemical bonding with the surface. Upon the irradiation of laser cleaning pulses, the particles absorb laser energy and cause thermal stresses in the particles [16]. The resulting stress could be large enough for the physical displacement, and hence removal of the particles from the surface. Furthermore, besides the above photo-thermal removal of the particles, photo-chemical reaction could also occur, resulting in the ablation and elimination of the particles by the laser, leaving behind a clean and undamaged surface. Figure 8 shows the comparison of a microfluidic channel surface with and without laser cleaning. The cleanliness of the quartz surface shows significant improvement. It demonstrates that the laser cleaning process can be incorporated into the microfluidic channel fabrication to

achieve in-situ dry cleaning using the same DPSS laser source.

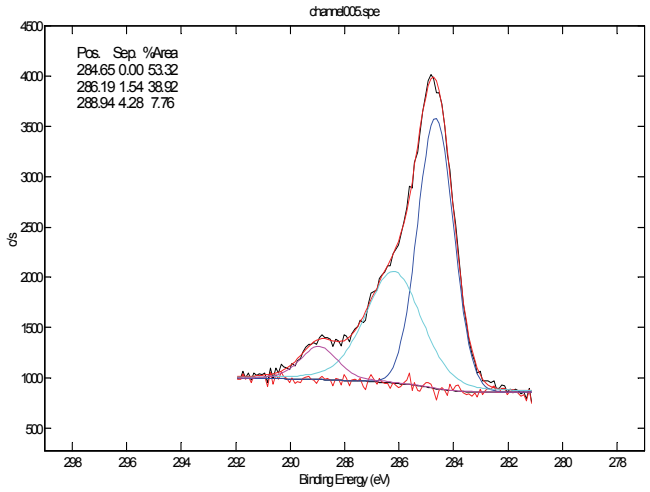

Fig. 7a. The binding energy of carbon is at 284.65 eV, 286.19 eV and 288.94 eV, which corresponds to C-C / C-H, C-O and C=O bonds, respectively.

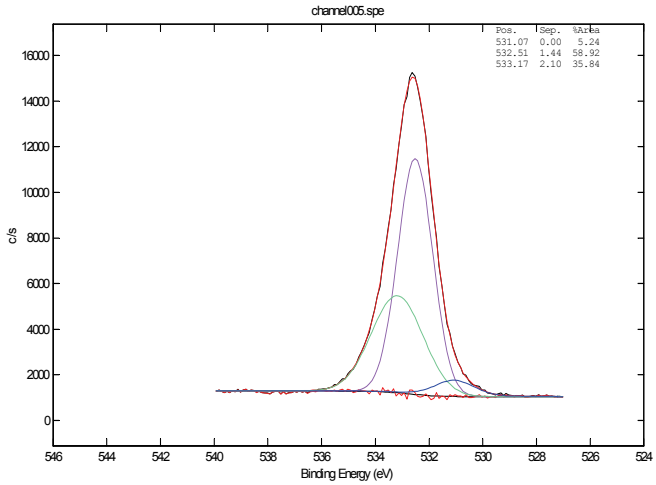

Fig. 7b. The binding energy of oxygen is at 532.51 eV and 533.17eV, which corresponds to O-Si / O-C and O=C bonds, respectively.

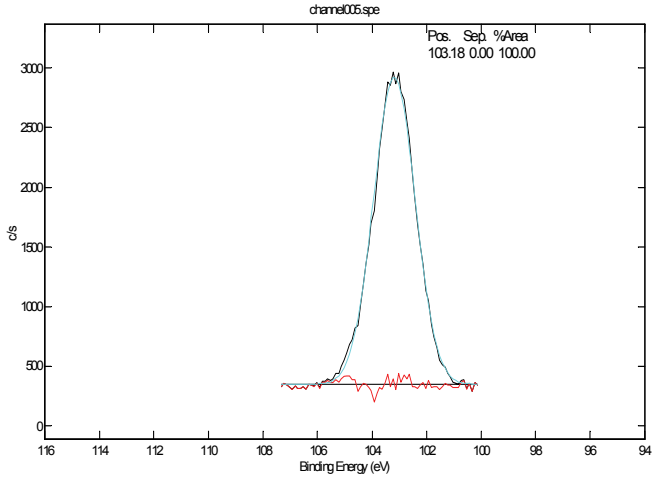

Fig. 7c. The binding energy at 103.18 eV is due to Si-O bonds, from the quartz composition.

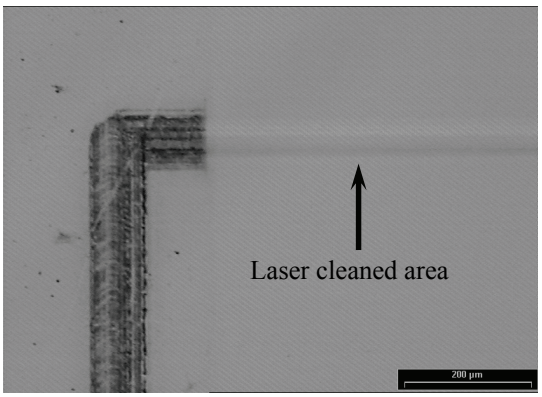

Fig. 8. Comparison between two substrate surfaces along the microfluidic channel with and without laser cleaning.

4. Conclusions

LIBWE is a promising technique to etch and fabricate micro-structures on quartz. High speed processing of the quartz surface using 355 nm DPSS Nd: YAG laser is demonstrated. The absorbing liquid plays an important role on the etch rate and the liquid with good absorption of the irradiating laser light yields a higher etch rate. At a laser fluence of 1.50 J/cm^2, the mixture of pyrene and toluene at a concentration of 0.4 M can yield an etch rate five times higher than using toluene alone. The relation between the etched depth and the laser fluence is non-linear. The increase in etched depth is more significant at a laser fluence of 1.42 J/cm^2 onwards. The threshold fluence in the mixture of pyrene and toluene is 0.4 J/cm^2, which is much lower than the threshold fluence of 1.1 J/cm^2 in toluene. By-products are formed after the LIBWE processing and are analyzed by XPS to be carbon. They can be subsequently removed using laser cleaning in air by the same laser but at a much lower laser fluence. High quality microfluidic channel structures can be created by this technique for biomedical applications. LIBWE can also be applied to fabricate micro-structures of different designs for other industrial applications.

Acknowledgments and Appendixes

We would like to thank Dr. G.X. Chen, Dr. L. Chan, Dr. C. M. Ng, Mr. S.K. Tan of Chartered Semiconductor Manufacturing, Singapore, for their invaluable advice and suggestion, and Ms Seek Chay Hoon of Data Storage Institute for her advice on XPS analyses.

References

[1] H. Varel, D. Ashkenasi, A. Rosenfeld, M. Wähmer, E.E.B. Campbell, Appl. Phys. A 65, (1997) 367-373

[2] M. Lenzner, J.Krüger, W.Kautek, F. Krausz, Appl. Phys. A 69, (1999) 465-466

[3] P.R. Herman, R.S. Marjoribanks, A. Oettl, K. Chen, I. Konovalov, S. Ness, Appl. Surf. Sci. 154-155, (2000) 577-586

[4] J. Wang, H. Niino, A. Yabe, Appl. Phys. A 68, (1999) 111-113

[5] J. Wang, H. Niino, A. Yabe, Appl. Surf. Sci. 154-155, (2000) 571-576

[6] H. Niino, Y. Yasui, X. Ding, A. Narazaki, T. Sato, Y. Kawaguchi, A. Yabe, J. Photochem. Photobiol. A-Chem. 158, (2003) 179-182
[7] R. Böhme, A. Braun, K. Zimmer, Appl. Surf. Sci. 186, (2002) 276-281
[8] J. Y. Cheng, M. H. Yen, C. W. Wei, Y. C. Chuang, T. H. Young, J. Micromech. Microeng. 15, (2005) 1147-1156
[9] Cs. Vass, B. Hopp, T. Smausz, F. Ignácz, Thin Solid Films 453-454, (2004) 121-126
[10] Cs. Vass, T. Smausz, B. Hopp, J. Phys. D-Appl. Phys. 37, (2004) 2449-2454
[11] J. Y. Cheng, M. H. Yen, T. H. Young, J. Micromech. Microeng. 16 (2006) 2420-2424
[12] H. Niino, Y. Kawaguchi, T. Sato, A. Narazaki, T. Gumpenberger, R. Kurosaki, J. Laser Micro /Nanoengineering, 1 (2006) 39-43
[13] Y.C. Tan, J.S. Fisher, A.I. Lee, V. Cristini, A.P. Lee, Lab. Chip, 4 (2004) 292-298
[14] P. B. Howell, Jr., D. R. Mott, S. Fertig, C. R. Kaplan, J. P. Golden, E. S. Oran, F. S. Ligler, Lap Chip, 5, (2005) 524-530
[15] H. Fukumura, H. Masuhara, Chem. Phys. Lett. 221, (1994) 373-378
[16] Y.F. Lu, W.D. Song, B.W. Ang, M.H. Hong, D.S.H. Chan, T.S. Low, Appl. Phys. A 65 (1997) 9-13

(Received: April 24, 2007, Accepted: September 6, 2007)